Am J Nucl Med Mol Imaging 2018;8(5):332-340
www.ajnmmi.us /ISSN:2160-8407/ajnmmi0081666

Original Article

Head to head comparison performance of ^{99m}Tc-EDDA/HYNIC-iPSMA SPECT/CT and ^{68}Ga-PSMA-11 PET/CT a prospective study in biochemical recurrence prostate cancer patients

Francisco Osvaldo García-Pérez[1], Jenny Davanzo[1], Sergio López-Buenrostro[1], Clara Santos-Cuevas[3], Guillermina Ferro-Flores[3], Miguel A Jímenez-Ríos[2], Anna Scavuzzo[2], Zael Santana-Ríos[2], Sevastián Medina-Ornelas[1]

[1]Nuclear Medicine and Department of Molecular Imaging, [3]Department of Urologic Malignances, Instituto Nacional de Cancerología, Mexico City, Mexico; [2]Department of Radioactive Materials, Instituto Nacional de Investigaciones Nucleares, Estado de México, Mexico

Received June 24, 2018; Accepted August 27, 2018; Epub October 20, 2018; Published October 30, 2018

Abstract: Positron emission tomography (PET) with prostate-specific membrane antigen (PSMA) has found widespread use for the diagnosis of biochemical recurrence of prostate cancer (PCa). Unfortunately, PET/CT is not as widely available; thus a PSMA-targeting compound for scintigraphy is of special interest. The aim of this study was to compare ^{99m}Tc-EDDA/HYNIC-iPSMA and ^{68}Ga-PSMA-11 PET/CT qualitatively and semi-quantitatively. Twenty-three patients with metastatic PCa were underwent ^{99m}Tc-EDDA/HYNIC-iPSMA SPECT/CT followed by ^{68}Ga-PSMA-11 PET/CT. Gleason score in all patients was obtained. Maximal standardized uptake value (SUVmax) and counts per organ, including the primary and metastatic tumor, were normalized and compared using Pearson's correlation test. Sites considered as positive have increased SUVmax and tumor-to-background ratio (TBR) in comparison with non-diseased organs/tissues (SUVmax =25.2±4.7, 18.4±1.6, 11.4±1.2 (P=0.037) from prostate, bone and lymph nodes versus TBR =35.9±45.2, 15.4±18.9, 19.1±51.7 (P=0.035) for prostate, bone and lymph nodes. ^{99m}Tc-HYNIC-iPSMA and ^{68}Ga-PSMA-11 uptake values in the evaluation of the affected nodes were very similar, although their ranges ranged from 5-21 mm (12±7.6). Correlation coefficient was normalized between SUVmax and TBR, demonstrating r values for prostate of r^2=0.731; for bone of r^2=0.720; and lymph nodes of r^2=0.864 (P<0.05 in all cases). Values and confidence interval at the 95% are supporting the equivalency of both parameters in primary tumor and metastases (prostate 95% CI=4.61, 4.38; bone tissue 95% CI=-2.21, 3.41 and lymph node 95% CI=4.67). We conclude that ^{68}Ga-PSMA-11 PET/CT and ^{99m}Tc-EDDA/HYNIC-iPSMA SPECT/CT were comparable, supporting the use of ^{99m}Tc-EDDA/HYNIC-iPSMA in patients with progressive metastatic castration-resistant PCa.

Keywords: ^{99m}Tc-HYNIC-PSMA, SPECT/CT, biochemical recurrence prostate cancer, ^{68}Ga-PSMA-11 PET/CT

Introduction

Prostate cancer (PCa) is the most common cancer in men and represents the third most common cause in cancer-associated deaths in men's. Early detection of primary disease is highly relevant in terms of prognosis and therapy management [1]. In Mexico PCa represents the most dominant malignant neoplasm in men among many others with highest incidence and mortality [2, 3]. Radical prostatectomy (RP) and radiotherapy (RT) are the main methods of treatment used in no metastatic disease. Despite of the optimal treatment, several patients developed biochemical failure or biochemical recurrence (BCR), i.e. a rise in prostate specific antigen (PSA) to above 0.2 ng/mL after RP, or >2 ng/ml in patients with locally advanced disease treated with external beam radiotherapy [4].

Among all available techniques, positron emission tomography (PET/CT) with choline-based radiotracers provides high sensitivity to primary lesion and some lymph node metastasis, although some authors have reported low specificity especially at low prostate-specific antigen (PSA) levels [5, 6]. Therefore, improved imaging

Table 1. Characteristics of the 23 Patients

Characteristic	Data
Age at scanning (y)	
Mean	68
Range	55-85
Gleason score	
6-7	2 (8%)
8-9	21 (92%)
PSA at scanning (ng/dl)	
Mean	80.85
Range	0.380-517
Risk group	
Intermediate	2 (8%)
High	21 (92%)
Previous treatment	
HT	17 (73%)
RT	5 (21%)
QT	8 (34%)
Ra-223	2 (8%)
None	2 (8%)

Abbreviations: HT = androgen deprivation therapy (including bicalutamide and LHRH); RT = radiotherapy; QT = chemotherapy (docetaxel); Ra-223 = radium-223. Data are followed by percentage in parentheses, except for age.

of PCa is necessary. In this context, it is reported that PET with ligands for the prostate-specific membrane antigen (PSMA) could overcome limitations of choline-based radiotracers.

PSMA is a membrane bound glycoprotein overexpressed in PCa. PSMA-targeted ligands labeled with gallium-68 (^{68}Ga), can show optimal detection of PCa recurrence especially in patients with low PSA levels. For instance, several studies recently observed that ^{68}Ga labeled Glu-CO-Lys(Ahx)-HBED-CC-PSMA (^{68}Ga-PSMA-11) increased detection rates in patients with biochemical recurrence after radical therapy, showing superior tumor-to-background (TBR) signal intensity and substantially higher detection rates compared with ^{18}F/^{11}C-Choline PET/CT [7-9].

Unfortunately, PET/CT is not as widely available, especially in low-income countries. Gamma cameras equipped with computed tomography (CT) it is still the equipment used in many nuclear medicine centers; thus a PSMA-targeting compound for scintigraphy is of special interest [10]. Importantly, evidence indicates that this hybrid imaging technology will become the gold standard for conventional scintigraphy for bone imaging performed for staging malignancy. Moreover, a remarkable advantage of this technique is that ^{99m}Tc-labeled tracers are much cheaper and more abundant than PET/CT tracers. In addition, a single elution obtainable from the ^{68}Ge/^{68}Ga generator is maximum for two doses per elution, which limits the number of patients per day [11].

Recent studies have demonstrated synthesis and biodistribution evaluation of ^{99m}technetium-EDDA/HYNIC-Lys(NaI)-Urea-Glu (^{99m}Tc-EDDA/HYNIC-iPSMA) in various clinical sites by SPECT/CT, and the acquired results showed highly sensitive detection of tumoral activity [12, 13]. This study addressed the ^{99m}Tc-EDDA/HYNIC-iPSMA clinical potential to evaluate primary disease and metastases. Here, we hypothesize that images produced with ^{99m}Tc-EDDA/HYNIC-iPSMA are qualitatively and semi-quantitatively comparable to images obtained with ^{68}Ga-PSMA-11 PET/CT. In order to test this hypothesis, visual comparisons and semi-quantitative correlations were conducted.

Material and methods

Study design and patients

Patients: Twenty three patients (age range: 55-85 years) were prospectively enrolled in this study from the Department of Urology in the National Cancer Institute (INCan) of Mexico. The inclusion criteria were biochemical recurrence with histologically diagnosed PCa. The study was approved by the Local Ethical Committee, and all participating patients signed an informed consent form. From January 2015 to august 2016, 23 patients underwent both ^{68}Ga-PSMA-11 PET/CT and ^{99m}Tc-EDDA/HYNIC-iPSMA within 1 week and in no particular order.

PSA median value was 80.85 ng/ml (range 0.380-517 ng/ml) and Gleason score in all patients ranged between 7 and 9. The administered activity to patients was 120-200 MBq of ^{68}Ga-PSMA-11 and 555-740 MBq of ^{99m}Tc-EDDA/HYNIC-iPSMA. Patient characteristics are summarized in **Table 1**.

Synthesis of ^{68}Ga-PSMA-11 & ^{99m}Tc-HYNIC-iPSMA

^{68}Ga was obtained from a ^{68}Ge/^{68}Ga generator (Isotope Technologies Garching) and Glu-CO-

Lys(Ahx)-HBED-CC (PSMA-11, GMP) was acquired from ABX Advanced Biomedical Compounds. The synthesis of ^{68}Ga-PSMA-11 was carried out on an iQS Ga-68 Fluidic Labeling Module (Isotope Technologies Garching). ^{99m}Tc-pertechnetate was obtained from a ^{99}Mo/^{99m}Tc generator (ININ-Mexico). Radiolabeling was performed by adding 1 mL of 0.2 M phosphate buffer (pH 7.0) to a HYNIC-iPSMA freeze-dried kit formulation (ININ-Mexico, GMP certificate), followed by immediately adding 555-740 MBq (1 mL) of ^{99m}Tc-pertechnetate and incubating at 95°C in a block heater for 10 min. The radiochemical purities of ^{68}Ga-PSMA-11 and ^{99m}Tc-EDDA/HYNIC-iPSMA- were >98% as determined by reversed-phase radio-HPLC.

Imaging protocol

Imaging was performed on a mCT Excel 20 PET/CT scanner (Siemens Medical Solutions). The acquisition parameters of the helical CT scan were 120 kVp, 180 mAs, and 5-mm slice thickness. After intravenous injection of ^{68}Ga-PSMA-11, whole-body emission scans were acquired at 60 min after injection. The whole-body PET scans were acquired from the vertex to mid thighs, at 2-3 min per bed position in 3-dimensional mode. PET images were reconstructed using a 2-dimensional ordered-subset expectation maximization algorithm. Regions of interest (ROIs) were drawn and the maximal standardized uptake value (SUVmax) of liver, spleen, duodenum, kidney, prostate, bone and lymph nodes, was obtained. The SUVmax was also obtained in all patients on a lesion-by-lesion basis. SUV measurements were performed side-by-side on corresponding lesions on fused image datasets. ROI's were drawn in gluteal muscles to obtain the reference SUVmax.

^{99m}Tc-EDDA/HYNIC-iPSMA SPECT/CT images were acquired at 3 h post tracer injection: the protocol used was a 360 degree rotation with a non-circular orbit continuous technique, 128x128 matrix, window of 15% centered on 140 keV with scattering correction, 120 images of 10 seconds in all acquisitions. CT images were acquired from the skull to the middle third of thighs, obtaining an attenuation correction map using low dose CT parameters. Reconstruction of raw data was carried out using the iterative method by the order of sets and subsets (8 iterations/4 subsets) and a Butterworth filter (cut 0.5, order 5). ROIs were drawn and the counts of liver, spleen, duodenum, kidney, prostate, bone, lymph nodes and lesions were obtained. A ROI was drawn in gluteal muscles to obtain the reference counts. The native counts of the organs were normalized to the counts of the gluteal reference.

Image analysis

The ^{68}Ga-PSMA-11 & ^{99m}Tc-HYNIC-iPSMA images were reviewed on a multimodality siemens workstation VG60, the ^{68}Ga-PSMA-11 SUVmax and TBR were measured by two experienced, independent nuclear medicine physicians. Each reader measured the same SUVmax and TBR lesion on both ^{68}Ga-PSMA-11 & ^{99m}Tc-HYNIC-iPSMA. Both reviewers used the interpretation criteria described by Rauscher, which consider as suspicious for malignancy any focal uptake of ^{68}Ga-PSMA-11 ligand higher than the surrounding background and not associated with physiological uptake, the same criteria was used for SPECT images. Nuclear medicine physicians were involved in interpretation, and that this was done by consensus. However, they later report kappa statistics, which is usually used to assess inter-observer agreement; the ICC rate was 0.911 (95% CI 0.903-0.989) for ^{68}Ga-PSMA-11 and 0.893 for ^{99m}Tc-HYNIC-iPSMA (95% CI 0.789-0.956). In both modalities the focal uptake was correlated with CT images. Lesion sites were divided into groups: bones, lymph nodes and prostate.

Statistical analysis

For statistical analysis, Pearson correlation test was performed using GraphPad Prism version 7.00 for Windows, GraphPad Software, La Jolla California USA, www.graphpad.com and Minitab version 17 were used. Normal distribution of continuous variables was confirmed by Kolmogorov-Smirnov test. Pearson's correlation test was conducted using z scores for SUVmax and tumor/no tumor ratio, which were obtained following the formula $X_{i,1\delta} = X_i\text{-}X_s/\delta_{x,s}$. SUVmax and tumor/no tumor ratio were used to perform the equivalence test, the corresponding standardized values were determined as follow:

ΔSUV (%) = (SUVmax1 - SUVmax2) × 100/SUVmax1

ΔT/TN (%) = (T/NT1 - T/NT2) × 100/T/NT1

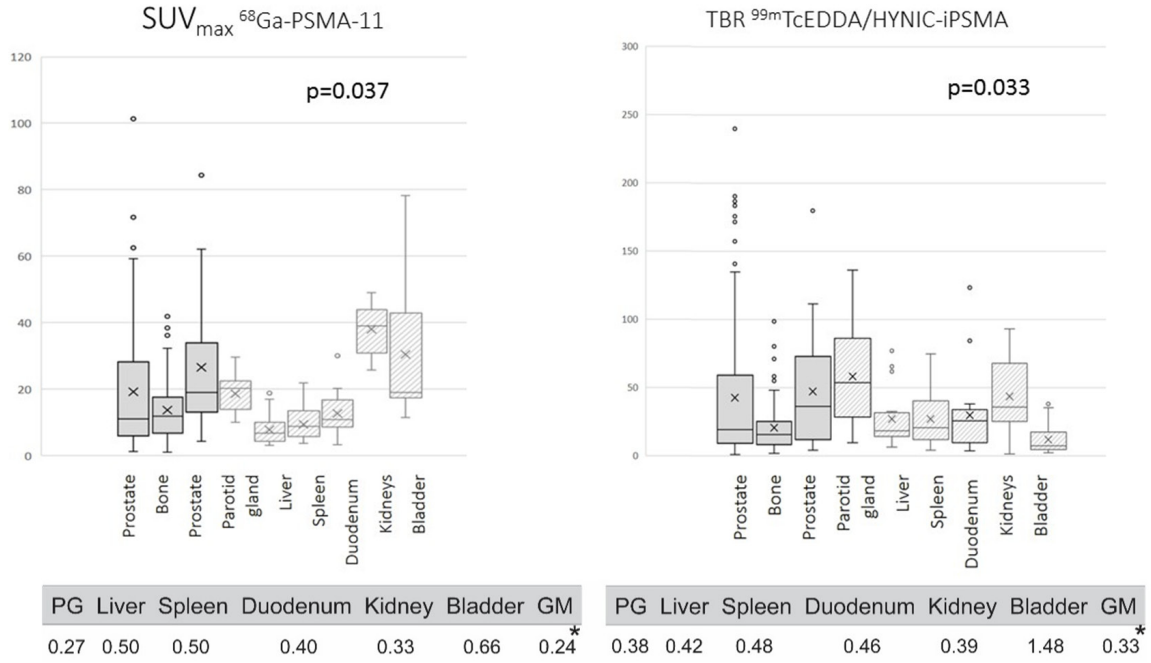

Figure 1. Sites considered as positive such as prostate gland, bone and lymph nodes have increased SUVmax and TBR in comparison with non-diseased organs/tissues (SUVmax =25.2±4.7, 18.4±1.6, 11.4±1.2 (P=0.037) from prostate, bone and lymph nodes (left) versus TBR =35.9±45.2, 15.4±18.9, 19.1±51.7 (P=0.035) for prostate, bone and lymph nodes (right).

Table 2. Coefficient of variation

	Prostate gland	Liver	Spleen	Doudenum	Kidney	Bladder
^{68}Ga-PSMA-11	0.27	0.50	0.50	0.40	0.33	0.66
^{99m}Tc-EDDA/HYNIC-iPSMA	0.38	0.42	0.48	0.46	0.39	1.48

Data are number of 23 patients with normal biodistribution findings evaluated with both studies.

Where SUVmax1 and TBR ratio represent uptake values for primary tumor and metastases, and SUVmax2 and TBR2 uptake per patients. Lastly, to evaluate whether SUVmax or TBR is the more stable parameter, we calculated the coefficient of variation of both variable (standard deviations divided by the respective average values). In all cases a *p* value of <0.05 was considered statistically significant.

Results

Biodistribution of ^{68}Ga-PSMA-11 and ^{99m}Tc-EDDA/HYNIC-iPSMA for non-diseased and diseased organs/tissues

According to SUVmax, all patients presented with a high radiotracer uptake in kidney (45.6± 3.4), following by bladder and parotid gland (28.5±4.2 and 19.5±2.4, respectively). Differences were noted when we compared SUVmax with TBR (**Figure 1**). In such case, highest uptake values were found in parotid gland and kidney (53.7±37.47 and 35.6±27.3, respectively) while bladder was one of the organs with a reduced TBR ratio (7.0±10.7). The lowest uptake was detected in gluteal muscle in both imaging tools (0.9±0.09 from PET/CT and 60.6±14 measured by number of counts from SPECT/CT). The coefficient of variation is showed in **Table 2** and it was lower for SUVmax reflecting more stable values when evaluating imaging.

Lastly, as it is observed in **Figure 1**, sites considered as positive such as prostate gland, bone and lymph nodes have increased SUVmax and TBR in comparison with non-diseased organs/tissues (SUVmax =25.2±4.7, 18.4±1.6, 11.4±1.2 (P=0.037) from prostate, bone and lymph nodes versus TBR =35.9±45.2, 15.4± 18.9, 19.1±51.7 (P=0.035) for prostate, bone

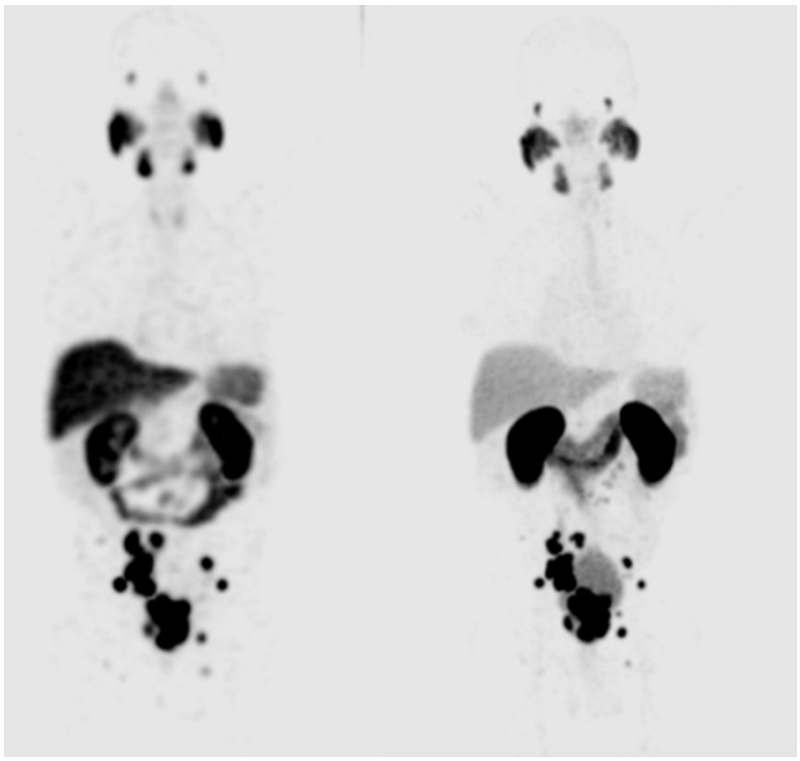

Figure 2. (left) Maximum-intensity projection of ^{99m}Tc-HYNIC-PSMA SPECT/CT. (right) Maximum-intensity projection of ^{68}Ga-HBED-CC PSMA.

and lymph nodes. Because literature indicates that an important but normal tracer uptake is seen in parotid glands, kidney and bladder by using ^{68}Gallium-labeled, these organs were excluded for comparison analysis.

Prostate or prostate bed was better visualized in the ^{99m}Tc-EDDA/HYNIC-iPSMA images, due to the time of acquisition of the study (4 h post injection) allows to obtain a greater urinary clearance of the radiotracer in bladder and a better tumor background ratio (**Figures 2** and **3**). There were no differences with both methods during the analysis of images in bone lesions, although there was a greater variation in the number of counts in bone lesions when compared to the SUVmax of the PET. Interestingly, the ^{99m}Tc-HYNIC-iPSMA and ^{68}Ga-PSMA-11 uptake values in the evaluation of the affected nodes were very similar, although their ranges ranged from 5 to 21 mm (12±7.6), with these results showing that the high relation Tumor-non tumor obtained by this radiopharmaceutical in images of 4 hours allows to identify nodes with metastatic affection even with normal dimensions.

^{99m}Tc-HYNIC-PSMA SPECT/CT is semi-quantitatively comparable with ^{68}Ga-PSMA PET/CT in both the primary tumor and metastases from bone and lymph nodes

SUVmax and TBR from primary tumor and positive bone and lymph nodes were recorded. Pearson correlation coefficient was used to assess the relation between normalized SUVmax and TBR. In all cases, a linear association between two variables were found. This is denoted in **Figures 4**-**6** by r and *p* values for prostate (r^2=0.731), bone (r^2= 0.720) and lymph nodes (r^2=0.864) (P<0.05 in all cases). Additionally, we conducted an equivalence test for demonstrating the comparability of both techniques. Hence, values and confidence interval at the 95% are supporting the equivalency of both parameters in primary tumor and metastases (Prostate 95% CI=4.61, 4.38; bone 95% CI=-2.21, 3.41 and lymph nodes 95% CI=4.67, 0). For equivalence test interval range -5% to 5% was selected because the uncertain of SPECT previously reported by other authors.

The SUVmax and TBR for the two tracers were compared within the 6 most typical regions: lymph nodes, bone, parotid glands, kidneys, bladder and prostate, for ^{68}Ga-PSMA PET/CT and ^{99m}Tc-HYNIC-PSMA SPECT/CT, and the results are shown in **Table 3**.

Lymph nodes analysis

In the lymph node analysis, we found an intense correlation between both methods in all sizes lymph nodes, but interestingly in the subgroup of lymph nodes smaller than 10 mm, the confidence in the interobserver analysis reach a Kappa of 0.950 SE ok 0.035 95% CI 0.882-1.000) for this analysis we studied 84 nodes in pelvic, retroperitoneal and inguinal regions, characterizing both reviewers 32 of 34 lymph

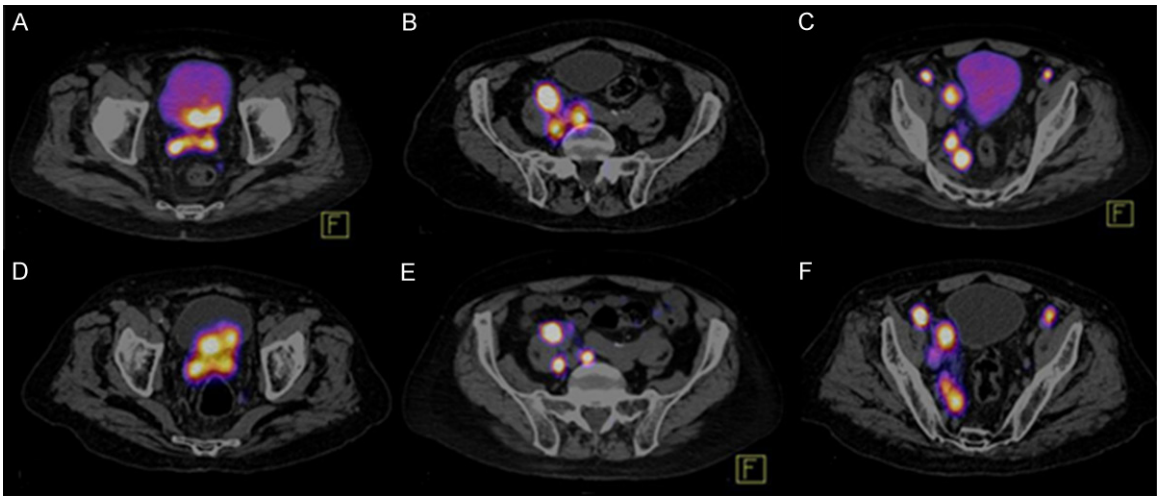

Figure 3. Comparison between ^{68}Ga-HBED-CC-PSMA PET/CT and ^{99m}Tc Hynic IPSMA SPECT/CT. A. Prostate tumor lesion that invades the wall of the bladder evaluate with ^{68}Ga-HBED-CC-PSMA PET/CT. D. ^{99m}Tc Hynic IPSMA show better target/background than ^{68}Ga-HBED-CC-PSMA PET/CT. B, C, E and F. Both methods detected retroperitoneal and pelvic lymph nodes, ^{68}Ga-HBED-CC-PSMA PET/CT and ^{99m}Tc-EDDA/HYNIC-iPSMA SPECT/CT with equal diagnostic accuracy.

nodes considered as positive by PET and 50 of 50 of negative lymph nodes.

Discussion

In the study of prostate cancer, a great variety of radiotracers have been used, mainly focused on the evaluation of metastatic disease such as bisphosphonates, after which ^{11}C-acetate or ^{11}C/^{18}F-choline tracers were used, which significantly improved the management of patients with BCR, however was the development of more specific molecules such as ligands targeting PSMA, which have changed the way to study patients with prostate cancer, at various stages from initial staging, follow-up and the response to therapy until recurrence [14-16].

There is scientific evidence robust enough to support the use of ^{68}Ga-PSMA inhibitors in these clinical scenarios. It has also been proposed to use these ^{18}F-labeled PSMA inhibitors [17]. However, there are sites in the world that do not count with a generator or cyclotrons with sufficient energy to produce ^{64}Cu, ^{89}Zr or ^{124}I which have also been used to label these molecules, but the requirement of complex systems of irradiation of solid target also becomes relatively complicated.

Clinical and preclinical studies using ligands or technetium-labeled PSMA inhibitors demonstrate a high affinity for neoplasic cells, but its efficiency had not been studied with respect to its counterpart with PET. Hiiler et al, demonstrated that of ^{99m}Tc-tricarbonyl-iPSMAcomplexes, showed a tumor uptake from 8.65% ID/g with ((7S,14S,18S)-7-amino-1-(1-(carboxymethyl)-1H-imidazol-2-yl)-2-((1-(carboxymethyl)-1H-imidazol-2-yl)methyl)-8,16-dioxo-2,9,15,17-tetraazaicosane-14,18,20-tricarboxylic acid) (MIP-1405 derivative) to 11% ID/g with ((7S,12S,16S)-1-(1-(2-(bis(carboxymethyl)amino)-2-oxoethyl)-1H-imidazol-2-yl)-2-((1-(2-(bis(carboxymethyl)amino)-2-oxoethyl)-1H-imidazol-2-yl)methyl)-9,14-dioxo-2,8,13,15-tetraazaoctadecane-7,12,16,18-tetracarboxylic acid) (MIP-1404 derivative) with a tumor-to-blood ratio from 33 (MIP-1405) to 550 (MIP-1404) and tumor-to-muscle from 72 (MIP-1405) to 157 (MIP-1404) at 4 h post-administration, corroborated with PSECT/CT imaging. In another study performed by Vallabhajosula et al showed that ^{99m}Tc-tricarbonyl-iPSMA biodistribution in humans does not correspond to preclinical data, because liver uptake is very high for MIP-1404 (around 18% ID at 4 h) with lower elimination (7%) than MIP-1405 (26%) at 4 h [18, 19].

Recently, Ferro-Flores et al developed a new radiopharmaceutical chemically defined as ^{99m}Tc-etilendiamine-N,N'-diacetic acid/hydrazinonicotinyl-Lys(Nal)-Urea-Glu (^{99m}Tc-EDDA/HYNIC-iPSMA) that targets PSMA; In vitro and in vivo studies showed high radiopharmaceutical

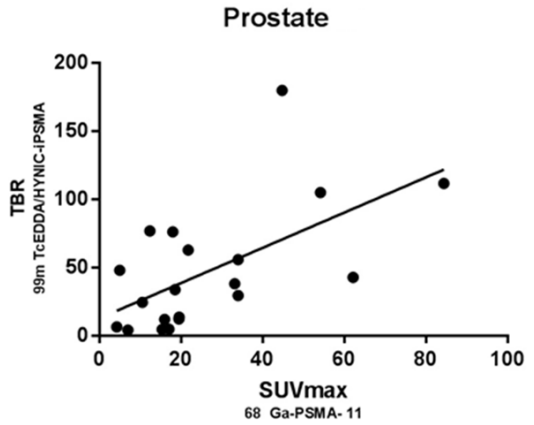

Figure 4. Scatter plot shows the correlation between normalized SUVmax of ^{68}Ga-PSMA-11 and TBR of ^{99m}Tc-HYNIC-PSMA SPECT/CT related uptake in prostate gland, which reaches statistical significance (rSpearman =0.594; P<0.05).

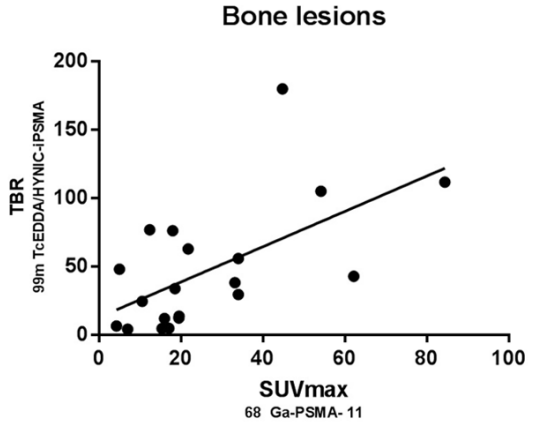

Figure 5. Scatter plot shows the correlation between normalized SUVmax of ^{68}Ga-PSMA-11 and TBR of ^{99m}Tc-HYNIC-PSMA SPECT/CT related uptake in bone metastatic disease, which reaches statistical significance (rSpearman =0.764; P<0.05).

stability in human serum, specific recognition for PSMA, high tumor uptake with rapid blood clearance and mainly kidney elimination. Preliminary images in patients demonstrated the ability of ^{99m}Tc-EDDA/HYNIC-iPSMA to detect tumors and metastases of prostate cancer, show a considerable less liver uptake than those obtained with MIP-1404 [12].

In this study, the found correlations between normalized values of SUVmax (^{68}Ga) and TBR (^{99m}Tc) from prostate (r^2=0.731), bone (r^2=0.720) and lymph nodes (r^2=0.864) demonstrated that ^{99m}Tc-EDDA/HYNIC-iPSMA is a promising radiopharmaceutical for targeting prostate cancer and performing site-specific imaging. Furthermore, a better correlation agreement between ^{68}Ga-PSMA-11 and ^{99m}Tc-EDDA/HYNIC-iPSMA is expected in all organs and lesions if SUVs are also applied for SPECT through a calibration of the system with phantoms containing different ^{99m}Tc activities and volumes. In a recent work Medina-Ornelas et al, showed strong correlation (P<0.05) between PSA levels in the same week of ^{68}Ga-PSMA-11 PET/CT performance (Trigger-PSA concept), but Trigger-PSA levels were not capable of distinguishing between localized or distant disease [20].

So far, we do not know a work that compares the image with PSMA inhibitors with both radionuclides. This emphasizes the importance of the results obtained in this work using ^{99m}Tc

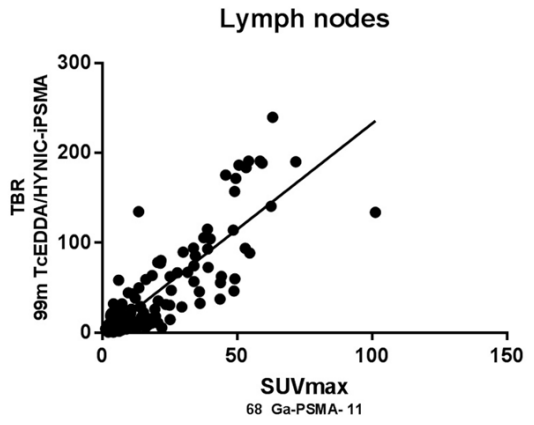

Figure 6. Scatter plot shows the correlation between normalized SUVmax of ^{68}Ga-PSMA-11 and TBR of ^{99m}Tc-HYNIC-PSMA SPECT/CT related uptake in lymph nodes, which reaches statistical significance (rSpearman =0.855; P<0.05).

Table 3. Comparison of SUVmax and T/NT for ^{68}Ga-PSMA PET/CT and ^{99m}Tc-HYNIC-PSMA SPECT/CT in the 23 Patients with PCa

Region	n*	SUVmax+	T/NT++	*p* value
Lymph nodes	138	12.6	21.1	<0.005
Bone	102	15.7	14.03	<0.005
Parotid glands	34	17.8	45.3	<0.005
Kidneys	34	37.2	30.41	0.2
Bladder	34	25.5	8.48	<0.005
Prostate	20	20.1	27.98	0.07

*Number of patients with regions available for measurement for both tumor lesion and normal corresponding tissue in both scans; +Mean of SUVmax values evaluated with ^{68}Ga-PSMA PET/CT; ++Mean of T/NT values evaluated with ^{99m}Tc-HYNIC-PSMA SPECT/CT.

EDDA/HYNIC-iPSMA as a SPECT/CT alternative as efficient as PET for the detection of tumor activity with overexpression of specific membrane antigen receptors of prostate.

In an interesting way, none of the lymph nodes in the data base of our study were referred at the celiac level, where it is known to show a relevant ^{68}Ga-PSMA uptake. In a study of Krohn et al at least one ganglion with ^{68}Ga-PSMA uptake was found in 89.4% patients which could mimic lymph node metastases [21].

Several centers use routinely the furosemide administration to enhance diuresis and improve image quality by reducing artifacts due to high activity of ^{68}Ga-PSMA ligand in the bladder and the urinary tract system, this would permit to improve the efficiency of detection of disease at the prostatic bed level. Rauscher et al, evaluate early recurrence of PCa, and they demonstrated that ^{111}In-PSMA I&T SPECT/CT detected 14 of 29 ^{68}Ga-PSMA PET/CT-positive lesions (48.3%) (correlation coefficient r= 0.6406; 95% confidence interval, 0.1667-0.8741; P=0.0136). There was no significant difference (P>0.05), but a weak trend toward a higher detectability in ^{111}In-PSMA I&T SPECT/CT regarding lesion size and initial PSA level [22].

Our study had some limitations. The lack of histopathological findings restricts the impact of these findings. Despite the small number of patients, it was reported that when patients were referred for follow up treatment, based on imaging results, their PSA decreased. Therefore, despite not being pathologically proven, the imaging results were true positives. Nevertheless, our main purpose was to see whether ^{99m}Tc-EDDA/HYNIC-iPSMA SPECT/CT could compete with the commonly used ^{68}Ga-PSMA-11 PET/CT, with lower cost and similar rate of detection of lesions.

Acknowledgements

We thank Nuclear Medicine Department at Instituto Nacional de Cancerologia, México. This research was carried out as part of the activities of the "Laboratorio Nacional de Investigación y Desarrollo de Radiofármacos-CONACyT".

Disclosure of conflict of interest

None.

Address correspondence to: Sevastián Medina-Ornelas, Department of Nuclear Medicine and Molecular Imaging, Instituto Nacional de Cancerología, México. Sevastián S. Medina Ornelas. Av. San Fernando, 22 Col. Sección XVI, Del. Tlalpan, C.P., Ciudad de México 14080, México. Tel: 0155 47471027 Ext. 10115; E-mail: dr.sevastian@outlook.com

References

[1] Siegel R, Ma J, Zou Z, Jemal A. Cancer statistics, 2014. CA Cancer J Clin 2014; 64: 9-29.

[2] Ferlay J, Soerjomataram I, Ervik M, Dikshit R, Eser S, Mathers C, Rebelo M, Parkin DM, Forman D, Bray F. GLOBOCAN 2012 v1.0, cancer incidence and mortality worldwide: IARC cancer base No. 11 [Internet]. Lyon, France: International Agency for Research on Cancer; 2013. Available: http://globocan.iarc.fr, accessed 20/Aug/2017.

[3] Erazo Valle-Solís Aura A, Aguilar-Melchor JM, Aguilar-Patiño S, Arce-Toledo C, Carvajal-Sánchez I, Ceballos-González S, Cepeda-López FR, Cervantes-Sánchez MG, Cortez-Betancourt R, Cruz-Rodríguez M, Enríquez-Aceves MI, Favela-Camacho JR, Fernández-Orozco A, Flores-Martínez M, Gatica-Pérez A, González-Hernández R, Güemes-Meza A, Hernández-Hernández C, Jáuregui-Chiu Mario G, Leal-Marroquín Ricardo A, Leos-Gallego CA, Mendoza-Peña F, Monzoy-Vásquez JO, Plascencia-García K, Ramírez-Corona E, Rodríguez-Zamudio MA, Romero-García P, Serna-Camacho ME and Velasco-Rodríguez JC. Reunión de panel de expertos en cáncer de próstata. Gaceta Mexicana de Oncología 2014; 13: 2-17.

[4] Roach M 3rd, Hanks G, Thames H Jr, Schellhammer P, Shipley WU, Sokol GH, Sandler H. Defining biochemical failure following radiotherapy with or without hormonal therapy in men with clinically localized prostate cancer: Recommendations of the rtog-astro phoenix consensus conference. Int J Radiat Oncol Biol Phys 2006; 65: 965-974.

[5] Schmid DT, John H, Zweifel R, Cservenyak T, Westera G, Goerres GW, von Schulthess GK, Hany TF. Fluorocholine PET/CT in patients with prostate cancer: initial experience. Radiology 2005; 235: 623-8.

[6] Umbehr MH, Müntener M, Hany T, Sulser T, Bachmann LM. The role of ^{11}C-choline and ^{18}F-fluorocholine positron emission tomography (PET) and PET/CT in prostate cancer: a systematic review and meta-analysis. Eur Urol 2013; 64: 106-117.

[7] Marchal C, Redondo M, Padilla M, Caballero J, Rodrigo I, García J, Quian J, Boswick DG. Expression of prostate specific membrane anti-

gen (PSMA) in prostatic adenocarcinoma and prostatic intraepithelial neoplasia. Histol Histopathol 2004: 19: 715-718.

[8] Afshar-Oromieh A, Avtzi E, Giesel FL, Holland-Letz T, Linhart HG, Eder M, Eisenhut M, Boxler S, Hadaschik BA, Kratochwil C, Weichert W, Kopka K, Debus J, Haberkorn U. The diagnostic value of pet/ct imaging with the ^{68}Ga-labelled PSMA ligand hbed-cc in the diagnosis of recurrent prostate cancer. Eur J Nucl Med Mol imaging 2015; 42: 197-209.

[9] Afshar-Oromieh A, Zechmann CM, Malcher A, Eder M, Eisenhut M, Linhart HG, Holland-Letz T, Hadaschik BA, Giesel FL, Debus J, Haberkorn U. Comparison of PET imaging with a ^{68}Ga-labelled PSMA ligand and ^{18}F-choline–based PET/CT for the diagnosis of recurrent prostate cancer. Eur J Nucl Med Mol Imaging 2014; 41: 11-20.

[10] Páez D, Orellana P, Gutiérrez C, Ramirez R, Mut F, Torres L. Current status of nuclear medicine practice in Latin America and the Caribbean. J Nucl Med 2015: 56: 1629-34.

[11] Nanabala R, Anees MK, Sasikumar A, Joy A, Pillai MR. Preparation of [^{68}Ga]PSMA-11 for PET-CT imaging using a manual synthesis module and organic matrix based ^{68}Ge/^{68}Ga generator. Nucl Med Biol 2016; 43: 463-9.

[12] Ferro-Flores G, Luna-Gutierrez M, Ocampo-Garcia B, Santos-Cuevas C, Azorín-Vega E, Jiménez-Mancilla N, Orocio-Rodríguez E, Davanzo J, García-Pérez FO. Clinical translation of a PSMA inhibitor for ^{99m}Tc-based SPECT. Nucl Med Biol 2017; 48: 36-44.

[13] Reinfelder J, Kuwert T, Beck M, Sanders JC, Ritt P, Schmidkonz C, Hennig P, Prante O, Uder M, Wullich B, Goebell P. First experience with SPECT/CT using a ^{99m}Tc-labeled inhibitor for prostate-specific membrane antigen in patients with biochemical recurrence of prostate cancer. Clin Nucl Med 2017; 42: 26-33.

[14] Ceci F, Uprimny C, Nilica B, Geraldo L, Kendler D, Kroiss A, Bektic J, Horninger W, Lukas P, Decristoforo C, Castellucci P, Fanti S, Virgolini IJ. ^{68}Ga-PSMA PET/CT for restaging recurrent prostate cancer: Which factors are associated with pet/ct detection rate? Eur J Nucl Med Mol imaging 2015; 42: 1284-1294.

[15] Husarik DB, Miralbell R, Dubs M, John H, Giger OT, Gelet A, Cservenyàk T, Hany TF. Evaluation of [^{18}F]-choline pet/ct for staging and restaging of prostate cancer. Eur J Nucl Med Mol Imaging 2008; 35: 253-263.

[16] Almeida FD, Yen CK, Scholz MC, Lam RY, Turner J, Bans LL, Lipson R. Performance characteristics and relationship of PSA value/kinetics on carbon-11 acetate PET/CT imaging in biochemical relapse of prostate cancer. Am J Nucl Med Mol Imaging 2017; 7: 1-11.

[17] Giesel FL, Cardinale J, Schäfer M, Neels O, Benešová M, Mier W, Haberkorn U, Kopka K, Kratochwil C. ^{18}F-Labelled PSMA-1007 shows similarity in structure, biodistribution and tumour uptake to the theragnostic compound PSMA-617. Eur J Nucl Med Mol Imaging 2016; 43: 1929.

[18] Vallabhajosula S, Nikolopoulou A, Babich JW, Osborne JR, Tagawa ST, Lipai I, Solnes L, Maresca KP, Armor T, Joyal JL, Crummet R, Stubbs JB, Goldsmith SJ. ^{99m}Tc-labeled small-molecule inhibitors of prostate-specific membrane antigen: pharmacokinetics and biodistribution studies in healthy subjects and patients with metastatic prostate cancer. J Nucl Med 2014; 55: 1791-98.

[19] Hillier SM, Maresca KP, Lu G, Merkin RD, Marquis JC, Zimmerman CN, Eckelman WC, Joyal JL, Babich JW. ^{99m}Tc-labeled small-molecule inhibitors of prostate-specific membrane antigen for molecular imaging of prostate cancer. J Nucl Med 2013; 54: 1369-76.

[20] Medina-Ornelas Sevastián S, García-Pérez Francisco O, Hernández-Pedro Norma Y, Arellano-Zarate Angélica E, Abúndiz-López Blanca L. Correlation between molecular tumor volume evaluated with ^{68}Ga-PSMA PET/CT and prostatic specific antigen levels. Rev Esp Med Nucl Imagen Mol 2018; 37: 223-228.

[21] Krohn T, Verburg FA, Pufe T. Neuhuber W, Vogg A, Heinzel A, Mottaghy FM, Behrendt FF. [^{68}Ga] PSMA-HBED uptake mimicking lymph node metastasis in coeliac ganglia: an important pitfall in clinical practice. Eur J Nucl Med Mol Imaging 2015; 42: 210-4.

[22] Rauscher I, Maurer T, Souvatzoglou M, Beer AJ, Vag T, Wirtz M, Weirich G, Wester HJ, Gschwend JE, Schwaiger M, Schottelius M, Eiber M. Intrapatient comparison of ^{111}In-PSMA I&T SPECT/CT and hybrid ^{68}Ga-HBED-CC PSMA PET in patients with early recurrent prostate cancer. Clin Nucl Med 2016; 41: e397-e402.